JOURNAL OF CATALYSIS 88, 431–447 (1984)

Rhodium Exchange in Zeolites

R. D. SHANNON,[1] J. C. VEDRINE, C. NACCACHE, AND F. LEFEBVRE

Institut de Recherches sur la Catalyse, CNRS 2, Avenue Albert Einstein, 69626 Villeurbanne Cedex, France

Received November 18, 1983; revised March 13, 1984

Rhodium exchange was attempted by using solutions of $RhCl_3$, $[Rh(NH_3)_5Cl]Cl_2$, and $Rh(ClO_4)_3$ in a series of zeolites with decreasing channel size: Y, mordenite, ZSM-34, ZSM-11, erionite, A, and ZK-5. Facile exchange was found in the large-pore zeolites Y and mordenite. Rh is found in the channels and on the surface of the medium-pore zeolites ZSM-34 and ZSM-11, suggesting that both exchange and surface hydrolysis occur. Surface hydrolysis to form islands of what is probably a Rh–oxy-hydroxy hydrate complex appears to be the primary type of deposition on the small-pore zeolites erionite, A, and ZK-5. Exchange in Y with the use of $RhCl_3(aq)$ solutions at 90°C, occurs via the $Rh(H_2O)_6^{3+}$ complex, does not result in an appreciable Cl^- concentration in the zeolite and, contrary to previous work, does not result in Rh on the external surface of the zeolite. Rh–Y prepared from $RhCl_3(aq)$ solutions can be used to prepare highly dispersed Rh in Y without the preliminary preoxidative treatment necessary for $Rh(NH_3)_5Cl$–Y. Reaction of CO with Rh-exchanged forms of Y, mordenite, ZSM-34, and ZSM-11 produces several species: $Rh(I)(CO)_2(O_z)_2$ in mordenite and Y; $Rh(I)(CO)_2(O_z)(H_2O)$ in all four zeolites; and $Rh(I)(CO)_3(O_z)$ in mordenite, ZSM-34, and ZSM-11.

INTRODUCTION

Zeolite ion exchange with trivalent ions is more difficult than with mono- or divalent ions because of the higher hydration energy of the small highly charged ions. Partial exchange has been reported with the trivalent ions of Co, Cr, Fe, Rh, Ti, Ru, Ir, In, Eu, Ce, and La in zeolites X, Y, L, mordenite, and ZSM-5 (*1–13*). Because small, highly charged cations tend to hydrolyze and give acidic solutions, exchange with these ions can result in partial lattice destruction of the zeolite (*4, 14*) and by interaction with the alkaline ions of the zeolite can form hydrolysis complexes or precipitates (*15, 16*).

Although Rh has been exchanged frequently into faujasite-type zeolites (*17–40*), very little effort has been expended to extend this exchange to other zeolites. The only other example of a Rh-exchanged zeolite is Rh–mordenite (*34*). This may be because of the bulky character of $[Rh(NH_3)_5Cl]^{2+}$ ($d = \sim 7.2$ Å), the ion generally used for exchange to keep the pH in the neutral range. We decided to investigate the feasibility of introducing the ions $[Rh(NH_3)_5Cl]^{2+}$ and $[Rh(H_2O)_{6-x}Cl_x]^{3-x}$ ($2 > x \geq 0$) into a series of zeolites with increasingly smaller channels. In addition to producing other Rh–zeolites, this would allow an empirical check of the size of various Rh complexes. The hexa-aquo ion, $Rh(H_2O)_6^{3+}$, was used to facilitate exchange and to minimize hydrolysis or precipitation. Exchange with $Rh(H_2O)_6^{3+}$ has the further advantage of avoiding the presence of Cl^- and NH_3 and might allow facile preparation of highly dispersed Rh particles <15 Å. Furthermore, Rh-exchanged zeolites with smaller channels would perhaps allow a certain degree of catalytic shape selectivity.

In this paper we describe attempts to exchange Rh into the zeolites Y, mordenite, ZSM-34, ZSM-11, erionite, A, and ZK-5 using solutions of rhodium(III) pentammine chloride, rhodium(III) chloride, and rhodium(III) perchlorate.

---

[1] On leave of absence from E.I. duPont de Nemours & Company, Central Research & Development Department, Wilmington, Del. 19898.

0021-9517/84 $3.00

EXPERIMENTAL

The zeolites Na–Y (LZY-52), Na–mordenite (M-5), NH_4–erionite (E-10), and Na–A (4A) were supplied by Union Carbide. ZSM-34, ZSM-11, and ZK-5 were prepared according to U.S. patents 4,086,186 (*41*), 3,709,979 (*42*) using tetrabutylphosphonium chloride, and 3,720,753 (*43*), respectively. Na–ZSM-34 and Na–ZSM-11 were prepared by exchange with 1 *N* NaCl from H–ZSM-34 and H–ZSM-11. NH_4–ZK-5 was analyzed for Na, K, Cs, Al, and Si and Na–ZSM-34 for Na, K, and Al by atomic absorption spectrometry. Total H_2O and ammonia contents were measured gravimetrically. The results were used for comparison with quantitative data obtained from X-ray photoelectron spectroscopy (XPS).

$[Rh(NH_3)_5Cl]Cl_2$ and $RhCl_3 \cdot xH_2O$ from Alfa Products were used in preparing the exchange solution; the identity and purity (>99%) of the pentammine were verified by ir spectra and X-ray diffraction. Several weak diffraction peaks indicated a minor amount of impurity (<1%). The $RhCl_3 \cdot xH_2O$ was analyzed by XPS to give Cl : Rh = 3.0 and O : Rh = 1.0.

Exchanges were carried out using 1 g zeolite/liter solution to minimize hydrolysis effects and to maximize the adsorption selectivity. Except for the mordenite exchange using $[Rh(NH_3)_5Cl]Cl_2$ sufficient Rh was added to the solutions to result in 2 wt% Rh (0.002–0.006 *M*). The mordenite-exchange solution contained enough Rh to introduce 12 wt% Rh (0.002 *M*). Exchanges were made by using $[Rh(NH_3)_5Cl]Cl_2$ solns and heating the solution to 80°C, adding the zeolite with rapid stirring, and continuing the exchange for 24 hr. The samples, after washed free of Cl^- ions with distilled H_2O and dried at 110°C, were colorless except for the erionite sample which was tan, probably because of Fe impurities.

Exchanges were carried out at 90°C using $RhCl_3$ solution. Ultraviolet spectra of a 0.002 *M* $RhCl_3$ solution at 90°C showed peaks at 380 and 475 nm which correspond to the species $Rh(H_2O)_3Cl_3$ reported by Wolsey *et al.* (*44*). Titration experiments of 0.005 *M* solutions with either NaOH or NH_4OH indicated precipitation beginning at ph ≅ 5.8. Initial pH values of the 0.002 *M* solutions were ~4; after exchange, the pH was 3.5–4.0.

Solutions which contained the complex $Rh(H_2O)_6^{3+}$ were prepared by prolonged digestion of 263 mg $RhCl_3 \cdot xH_2O$ in 20 ml 10 *M* $HClO_4$ (*45*). The solution diluted to 0.05 *N* was yellow. A uv spectrum of 0.005 *N* solution showed peaks at 310 and 400 nm and thus corresponded well to $Rh(H_2O)_6^{3+}$ (*44*). Titration experiments of 0.01 *M* soln with 0.1 *M* NaOH resulted in turbidity beginning at pH ~ 4.4 in agreement with Forrester and Ayres (*46*) and Jørgensen (*47*). Exchange experiments using perchlorate solutions of $Rh(H_2O)_6^{3+}$ were carried out by adjusting the pH to 3.7 with NaOH, heating to 70°C, adding the zeolite, and stirring for 6 hr.

After the exchanges were done all samples were washed-free of Cl^- with distilled H_2O and dried at 110°C. The colors of the samples exchanged in either the chloride or perchlorate solutions ranged from light yellow to pinkish tan.

An attempt to exchange Na–A with $Rh(H_2O)_6^{3+}$ failed. The exchange solution was 0.00024 *M* Rh perchlorate with sufficient NaOH added to make the pH 3.2. When a sample of Na,H–A, prepared by prehydrolysis in H_2O, was added to this solution at 70°C, the pH jumped immediately to 6.0. After stirring at 70°C for 6.5 hr, the pH was 7.4. When this sample was dried at 110°C, in contrast to the other Rh-exchanged samples, it turned brown. Because precipitated $Rh(OH)_3$ also turns brown at 110°C, it was assumed that $Rh(OH)_3$ was precipitated on the exterior of the Na–A crystallites.

After exchange the Na and Rh contents were determined by atomic absorption techniques. The relative crystallinity was determined by comparing intensities of the peaks in the X-ray diffraction patterns of the exchanged samples with those of the unexchanged samples. Diffuse reflectance spectra of the samples dried at 110°C were obtained using an Optica CF4 Ni spectrophotometer using MgO as a reference. Infrared spectra were obtained in the range 200–4000 cm^{-1} on a Perkin–Elmer 580 spectrophotometer. KBr and self-supporting disks were prepared according to a procedure already described (*48*).

XPS was used to ascertain the distribution of Rh between the zeolite interior and exterior surfaces. The XPS experiments were performed with a Hewlett–Packard 5950A spectrometer using monochromatized Al$K\alpha$ radiation. The samples were pressed into a sample holder using In foil and introduced into the sample chamber at 10^{-8} Torr. Spectra were recorded at room temperature using a multichannel computer analyzer. The data were analyzed using a computer program to smooth the peaks, determine the area, and subtract the background. Quantitative analysis was performed using the relationship

$$\frac{n_1}{n_2} \cong \frac{A_1}{A_2} \frac{\sigma_2 E_{K_2}^{1/2}}{\sigma_1 E_{K_1}^{1/2}}$$

where A = peak area, E_K = the kinetic energy, and σ = the effective cross section calculated by Scofield (*49*). The Si/Al ratios determined in this manner for zeolites agreed well with those determined by chemical analysis. The standards NaCl, $[Rh(NH_3)_5Cl]Cl_2$, and $Rh_2Cl_2(C_8H_{12})_2$ (see Table 2), were used to correct the Cl/Rh, N/Rh, and Na/Si values using the experimental Cl/Rh, N/Rh, and Na/Cl values and the above relationship. The values in Table 2 (A, B, and C) were obtained by multiplying by the factors 0.88, 1.15, and 0.50, respectively. The Rh $3d_{5/2}$ and N $1s$ binding energies were corrected assuming *BE* (Si $2s$) = 154.0 eV.

Surface to bulk metal contents were evaluated using Rh/Si ratios determined from XPS and from bulk chemical analysis (labeled XPS and CA, respectively, in Tables 2 and 3). The XPS/CA ratios were used to obtain a qualitative indication of the amount of Rh on the external surface of the zeolite grains (*36*).

Infrared studies of the interaction between CO and the Rh-exchanged zeolites were carried out using self-supporting disks. The disks weighing ~10 mg and measuring 18 mm in diameter were pressed at 1000 kg-cm^{-2} and introduced into a specially designed cell (*25*) with a greaseless stopcock. Samples exchanged with either $RhCl_3$(aq) or $Rh(H_2O)_6^{3+}$ were first heated under vacuum for 6 hr at 150°C to eliminate H_2O. After 10 Torr CO was added, the samples were heated successively for 18 hr at 100°C and 24 hr at 200°C and spectra were obtained after each stage. In order to eliminate NH_3 and Cl from samples exchanged with $Rh(NH_3)_5Cl^{2+}$, the samples were heated slowly to 300°C in O_2 over a period of 18 hr, then under a vacuum at 300°C for 5 hr. CO was then introduced and the heating was performed in the same manner as the other samples.

H_2 chemisorption experiments were carried out on reduced Rh–Y samples to determine the degree of dispersion. The Rh$(NH_3)_5$Cl–Y samples (500 mg) were heated (0.2°C/min) to 300°C in O_2 (5 liters/hr) in a cell 2 cm in diameter, evacuated at 300°C, cooled to room temperature, and heated (3°C/min) under H_2 (3 liters/hr) to various temperatures. The Rh–Y samples prepared from $RhCl_3$(aq) and $Rh(ClO_4)_3$(aq) were evacuated at 200°C overnight before H_2 reduction at various temperatures.

Hydrogen adsorption measurements were carried out in a conventional glass vacuum apparatus. Hydrogen pressures in the range 10–200 Torr were measured using a Texas Instruments precision pressure gauge. About 0.5 g of the supported rhodium sample was placed in a U-shaped flow-through reactor and subjected to the pretreatment procedure described above. Before hydrogen adsorption, the reduced samples were evacuated at 400°C for 2 hr.

Hydrogen adsorption was carried out at room temperature. Samples were allowed to equilibrate at ~100 Torr H_2 pressure after which the H_2 adsorption isotherms were determined between 50 and 200 Torr. The samples were then evacuated at 22°C and a second adsorption isotherm (back sorption) determined, which by extrapolation to zero pressure provided the reversibly bound hydrogen. The difference between the first and the second isotherms gave the amount of hydrogen strongly bound to rhodium. The metal dispersion was derived from the quantity of irreversibly adsorbed hydrogen assuming a stoichiometry of $H/Rh_s = 1$. The metal dispersion is given by $D\% = 100 \times Rh_s/Rh_t$ where Rh_s corresponds to rhodium surface atoms derived from H_2 adsorption and Rh_t, the total number of rhodium atoms derived from chemical analysis.

RESULTS

1. Exchange with $[Rh(NH_3)_5Cl]Cl_2$ *Solutions*

Tables 1 and 2 summarize the analytical data for pentammine rhodium chloride exchange. Only mordenite and Y show facile exchange. XPS/CA ratios for these two zeolites indicate that all of the Rh is located in the interior of the grains. Higher XPS/CA ratios and lower degrees of exchange for ZSM-34 and ZSM-11 show that although the pentammine ion enters the channels, some is adsorbed on the zeolite exterior surfaces. The Si + Al/O ratio determined by XPS is also an indication of surface Rh; it is expected to be less than 0.5 if some Rh is found on the surface. The slightly decreased values 0.45 and 0.48 for ZSM-34 and ZSM-11 are consistent with the increased XPS/CA values. The Rh pentammine ion is obviously too large to enter 4-Å channels. The very low quantities of Rh found in erionite and ZK-5 are believed to result from surface exchange or hydrolysis. This assumption is supported by the relation between the quantities of Rh exchanged and the surface areas of erionite and ZK-5.

The Cl/Rh values are all less than 1, as anticipated from the use of dilute solutions of Rh pentammine chloride at 80–90°C (*50*). The equilibrium ratios of $[Rh(NH_3)_5Cl]^{2+}/[Rh(NH_3)_5H_2O]^{3+}$ in soln were found by Lamb to be proportional to the Rh concn (*50*) and our experimental values in the zeolites agree with this observation. The lower

TABLE 1

Bulk Rh Content of Rh-Zeolites

Zeolite	Channel dimensions[a]	% Rh Using		$Rh(H_2O)_6^{3+}$	Typical particle size (μm)	External surface area (m²/g)
		$Rh(NH_3)_5Cl^{2+}$	$RhCl_3$			
Na–Y	7.4***	2.61	2.37	1.93	0.3–0.7	
Na–mordenite	6.7 × 7.0* ↔2.9 × 5.2*	4.91	1.47	1.38	0.5–1.0	30
Na–ZSM-34	3.6 × 5.2** ↔6.4*	0.73	1.30	1.41	0.3–0.7	63
Na–ZSM-11	5.1 × 5.5***	0.46	1.61	0.87	0.5–1.0	14
NH_4–erionite	3.6 × 5.2***	0.13	0.73	0.62	1–5	11
Na–A	4.1***		1.25		1–3	4
NH_4–ZK-5	3.9***	0.26	1.31	0.80	0.7–0.9	26

[a] The number of asterisks used indicates whether the channel system is one-, two-, or three-dimensional. Interconnecting channel systems are separated by a double arrow. W. M. Meier and D. H. Olson, "Atlas of Zeolite Structure Types." J. Druck Verlag AG, Zurich, Switzerland, 1978.

TABLE 2

XPS Data on Rh-Exchanged Zeolites

	% Rh	Rh_{3d}/Si_{2s}		XPS/CA	Si_{2p}/Al_{2p}		Cl_{2p}/Rh_{3d}		Cl_{2p}/Si_{2s}		N_{1s}/Rh_{3d}	$\frac{Si + Al}{O}$	Na_{1s}/Si_{2s}	
		XPS	CA		XPS	CA	XPS	CA	XPS	CA			XPS	CA
A. Exchange with $[Rh(NH_3,H_2O)_5 H_2O,Cl]^{n+}$														
Na–Y (.0005 *M* Rh)	2.61	.028	.025	1.1	2.60	2.43	.21	.122	.005	.006	2.6	.50	.31	.28
Na–mordenite (.0025 *M*)	4.91	.043	.040	1.1	5.6	5.0	.44		.02		4.7	.51	.10	.08
H–ZSM-34 (.006 *M* Rh)	0.73	.010	.006	1.7	6.9		.71		.007		7.0	.45	.002	
Na–ZSM-11 (.002 *M* Rh)	0.46	.016	.004	4.0	18.6	20.1	.37		.009			.48	.003	
B. Exchange with $RhCl_3$(aq)														
Na–Y	2.37	.023	.023	1.0	2.54	2.43	.12	.14	.003	.006		.49	.35	.34
Na–mordenite	1.47	.037	.012	3.1	5.00	5.00	.10		.004			.50	.15	.14
Na–ZSM-34	1.30	.017	.013	1.4	4.80	5.10	.00		.00			.46	.01	.011
Na–ZSM-11	1.61	.07	.014	5.0	14.4	20.1	.03		.003			.44	.02	.014
NH_4–erionite	0.73	.25	.007	35	4.4	—	.13		.04			.40	.001	
Na–A	1.25	1.33	.022	60	0.90	1.00	.11	.30	.160	.007		.23	.57	
NH_4–ZK-5	1.31	0.27	.013	21	3.90	3.56	.12	.24	.030	.003		.38		
C. Exchange with $Rh(H_2O)_6^{3+}$														
Na–Y	1.93	.018	.019	1.0	3.4	2.43	.19		.004			.45	.023	.07
Na–mordenite	1.38	.013	.011	1.1	5.4	5.0	.90		.010			.49	.13	.124
Na–ZSM-34	1.41	.027	.011	2.4	7.4	5.10	.00		.00			.46	.018	.024
Na–ZSM-11	0.87	.034	.008	4.2	18.3	20.1	.42		.013			.49	.05	.024
NH_4–erionite	0.62	.18	.006	30.0	4.6		.04		.009			.50	.003	
NH_4–ZK-5	0.80	.11	.008	13.8	3.1	3.56	.03	.256	.003	.002		.46	.003	
D. Standards														
Na–mordenite					5.3				.012			.47		
(theoretical)					(5.0)							(.50)		
$Rh_2Cl_2(C_8H_{12})_2$ Rh/C = 0.11							1.02							
(theoretical) (.12)							(1.00)							
$Rh(NH_3)_5Cl_3$ Cl/N = (.57)							2.43				5.00			
(theoretical) (.60)							(3.00)				(5.00)			
NaCl Cl/Na = 1.00														
(theoretical) (1.00)														

quantities of Cl found in the zeolites compared with those in solution (Lamb found Cl/Rh = 0.87 for 0.005 *M* at 84°C) are probably caused by replacement of Cl^- by OH^- resulting from exchange with zeolite Na^+ or NH_4^+ ions. It is clear, however, that at RT Cl accompanies the Rh pentammine ion in more concentrated solutions (*25*) and remains coordinately bonded to Rh to form $[Rh(NH_3)_5Cl]^{2+}$ ions.

2. $RhCl_3(aq)$ Exchange

Only zeolite Y shows facile exchange in $RhCl_3$ solutions at 90°C. The XPS/CA ratio for Na–ZSM-34 of 1.4 indicates only a small amount of Rh at the external zeolite surface. Mordenite and Na–ZSM-11 show somewhat more Rh at the external surface. Erionite, A, and ZK-5 channels are obviously too small to allow entry of the hydrated Rh species and most or all of the Rh is deposited at the external surface as evidenced by XPS/CA ratios of 35, 60, and 21, respectively. Correspondingly the apparent Si + Al/O ratios deviate significantly from 0.50. Despite the fact, however, that Rh is being deposited at the surface and not exchanged, the NH_4^+ and Na^+ content of the zeolites have been diminished considerably as evidenced by chemical analysis of Rh, Na–A and ir spectra of Rh,NH_4–erionite and Rh,NH_4–ZK-5. This reduction in Na^+ and NH_4^+ may occur via exchange with protons.

Cl/Rh ratios in the zeolites exchanged in $RhCl_3$(aq) are not appreciably greater than 0.10. This is confirmed by both XPS and CA (see Table 3). Thus the Cl does not accompany the Rh ion during the exchange at 90°C. Cl/Si ratios in the exchanged zeolite are of the same order of magnitude as in the starting materials (Table 3) except for Rh, Na–A and Rh,NH_4–ZK-5 where the Cl seems to be concentrated in the outer surfaces along with the Rh. It is possible that the Cl is present in a hydrolysis product but is partially removed during the washing.

3. $Rh(H_2O)_6^{3+}$ Exchange

Again both zeolite Y and mordenite show facile exchange. ZSM-34 and ZSM-11 exchange is similar to that in $RhCl_3$(aq) with Rh both in the channels and on the external surface but ZSM-11 has exchanged only half as much Rh. High XPS/CA ratios for both ZK-5 and erionite suggest that most of the Rh has deposited on the external surfaces. By comparison with $RhCl_3$(aq) exchange, only half as much Rh has deposited on ZK-5. Qualitatively, exchange in $Rh(H_2O)_6^{3+}$ solutions is not very different than exchange in $RhCl_3$(aq) solutions at 90°C. However, because of the lower solution pH, the surfaces of both Y and ZSM-34 are deficient in Al.

The lower Na content of the Y sample exchanged in $Rh(H_2O)_6^{3+}$ solutions is probably a result of the lower pH. However, the Na content of mordenite, and ZSM-11, and the NH_4 content of erionite and ZK-5 do not seem to be affected by the lower pH. The lower pH probably also is responsible for less hydrolysis product on ZK-5.

The Cl contents of these zeolites differ from those for $RhCl_3$(aq)-exchanged samples. Although Y and ZSM-34 remain unchanged, mordenite and ZSM-11 appear to have retained more Cl^- through the presence of ClO_4^- than Cl^- in $RhCl_3$(aq). Erionite and ZK-5, with Rh at the surface, have picked up less Cl^-.

4. Rh $3d_{5/2}$ and N 1s Binding Energies

Table 4 shows that the Rh $3d_{5/2}$ binding energies are 310–311 eV, in good agreement with other studies (*25, 30, 31, 34, 51–53*). However, there appears to be a systematic difference between the Rh pentammine-exchanged samples ($BE_{av} \cong$ 311 eV) and the samples exchanged with either $RhCl_3$(aq) or $Rh(H_2O)_6^{3+}$ ($BE_{av} \cong$ 310 eV). It is perhaps not surprising the Rh^{3+} coordinated by NH_3 ligands might have slightly different binding energies than Rh^{3+} coordinated by H_2O but it should be noted that $[Rh(NH_3)_5Cl]^{2+}$–Y samples as ex-

TABLE 3

Results of Cl Analyses

Zeolite	Exchange	Cl/Rh		Cl/Si		Comments
		XPS	CA	XPS	CA	
Na–Y	$[Rh(NH_3)_5Cl]^{2+}$	.2	.12	.005	.006	Cl evenly distributed throughout zeolite with Rh; probably entered zeolite as mixture of $[Rh(NH_3)_5Cl]^{2+}$ and $[Rh(NH_3)_5H_2O]^{3+}$
Na–Y	$RhCl_3$	.1	.14	.003	.006	Cl evenly distributed throughout zeolite; probably entered zeolite as mixture of $Rh(H_2O)_5Cl]^{2+}$ and $[Rh(H_2O)_6]^{3+}$
Na–A	$RhCl_3$	.11	.30	.16	.007	Cl not in interior of grains; associated with Rh at surface (from Cl/Si ratio); Cl is leached from outer surface (from Cl/Rh ratio)
NH_4–ZK-5	$RhCl_3$	.12	.24	.03	.003	Same comments as Na–A/$RhCl_3$
	$Rh(H_2O)_6^{3+}$	.03	.25	.003	.002	Cl distributed even through grains and not associated with Rh at surface
NH_4–ZK-5	None				.003	Most of the Cl found in Rh–ZK-5 was present in the original sample and not introduced during exchange process
Na–Y	None				.005	Most of the Cl found in Rh–Y ($RhCl_3$ and $Rh(NH_3)_5Cl_3$) was present in the original sample and not introduced during exchange
Na-mordenite	None			.010	.003–.005	Some Cl introduced into Rh-mordenite during exchange in $Rh(NH_3)_5Cl_3$ and $Rh(H_2O)_6^{3+}$ but not during exchange with $RhCl_3$

changed and treated at 400–500°C in O_2, presumably resulting in Rh_2O_3–Y, were found by Anderson and Scurrell (*34*) and Primet *et al.* (*25*) to have the same Rh *BE*'s.

Samples exposed to the X-ray beam for extended periods of time showed peaks at lower binding energies as noted by Anderson and Scurrell and Anderson *et al.* (*34, 51*). In general these peaks were found at *BE*'s of 308–309 eV, generally believed to be characteristic of Rh(I) (*51*). The samples prepared by $Rh(H_2O)_6^{3+}$ exchange were more strongly reduced than the others.

N 1*s* *BE*'s of 401–402 eV in $[Rh(NH_3)_5Cl]^{2+}$–zeolites and $[Rh(NH_3)_5Cl]Cl_2$ clearly represent NH_3 ligands surrounding Rh^{3+} ions and are in good agreement with data on $Pt(NH_3)_2Cl_2$ and $Pt(NO_2)_2(NH_3)$, 400.4 and 400.1 eV, respectively (*52*). This is confirmed by strong NH_3 ir bands at 1310 cm^{-1} and N–H bands at 3250 cm^{-1}. These samples are also characterized by weak peaks at 402–403 eV which probably derive from NH_4^+ formed during decomposition of the $[Rh(NH_3)_5Cl]^{2+}$ ion in solution and subsequent exchange into the zeolite. The presence of NH_4^+ is indicated by ir bands at 1410 cm^{-1}.

With the exception of erionite, all samples exchanged in $RhCl_3$(aq) and $Rh(H_2O)_6^{3+}$

TABLE 4

Rh $3d_{5/2}$ Binding Energies

Zeolite	Binding energies (eV) Rh $3d_{5/2}$[a]	
	(1)	(2)
$Rh(NH_3)_5Cl$, H_2O exchange		
Na–Y	311.3[10]	309.3[7]
Na–mordenite	311.1[10]	308.0[4]
Na–ZSM-34	310.3	
Na–ZSM-11		308.8
$RhCl_3$(aq) exchange		
Na–Y	310.3	
Na–mordenite	309.7	308.0
	310.2	308.4
Na–ZSM-34	310.0	
Na–ZSM-11	309.6	308.4
	310.0[10]	308.4[3]
NH_4–erionite	309.9	
Na–A	310.7	
NH_4–ZK-5	310.0[10]	308.2[3]
$Rh(H_2O)_6^{3+}$ exchange		
Na–Y	310.5[10]	308.7[8]
Na–mordenite		308.7
Na–ZSM-34	310.3[10]	309.1[8]
Na–ZSM-11	309.7[8]	307.9[10]
NH_4–erionite	309.7	
NH_4–ZK-5	311.0[8]	309.4[10]

[a] Rh $3d_{5/2}$ binding energies referenced to Si_{2s} at 154.0 eV. (1) Rh $3d_{5/2}$ for Rh^{3+}; relative intensity in brackets. (2) Rh $3d_{5/2}$ from Rh^{3-n} reduced by X-ray beam; relative intensity in brackets.

solutions contained distinct peaks at ~402–403 and ~400–401 eV with intensity ratios of from 0.5 : 1 to 1 : 0.8. Although N/Si by XPS ≅ 0.03–0.05, bulk chemical analyses showed N/Si ratios <0.001. Thus the N XPS signals originate from an unknown surface N species.

5. *Diffuse Reflectance Spectra*

All samples exchanged in $RhCl_3$(aq) or $Rh(ClO_4)_3$(aq) solutions and dried at 100°C showed a strong band at ~260 nm and a weaker broad band at 440 nm, in agreement with the spectra found by Okamoto *et al.* (*30*). There was no apparent difference between samples such as Rh–Y showing facile exchange and Rh–ZK-5 in which the Rh is found at the external surface.

6. *H_2 Chemisorption on Rh–Y*

Highly dispersed samples of Rh in Y zeolite have previously been prepared from $Rh(NH_3)_5Cl$–Y by a preoxidative treatment at 300–350°C followed by H_2 reduction at 300°C (*24, 55*). Because Rh–Y prepared from $RhCl_3$(aq) solutions contains only H_2O, OH^-, or O^{2-} ligands, it should be possible to produce highly dispersed Rh^0 without the preoxidation step. Table 5 shows the results of H_2 chemisorption experiments performed on 2% Rh–Y samples prepared from $[Rh(NH_3)_5Cl]Cl_2$, $RhCl_3$(aq), and $Rh(ClO_4)_3$(aq) solutions. The Rh–Y produced from $Rh(NH_3)_5Cl$–Y gives good dispersion over a temperature range of 220–530°C, as shown by previous experiments (*24, 55*). A dispersion of 90% was found for the $RhCl_3$(aq) sample after reduction at 225°C. Further heating in H_2 at 425°C reduces the dispersion to 55%. The sample prepared from $Rh(ClO_4)_3$(aq) did not give dispersions greater than 65%. The poorer dispersion of this sample may be related to the poorer crystallinity of this sample.

7. *Interaction of Rh–Zeolites with CO*

All samples showed characteristic carbonyl spectra with bands in the region 2000–2200 cm^{-1} (Fig. 1) which were different for each zeolite but did not depend on

TABLE 5

Rh Dispersion on Rh–Y Samples

Rh–Y sample from	T(°C) of H_2 reduction	Dispersion, %
$[Rh(NH_3)_5Cl]Cl_2$(aq)	220	76
2.61% Rh	400	74
$RhCl_3$(aq)	150	61
2.37% Rh	225	92
	425	55
$Rh(ClO_4)_3$(aq)	150	65
1.93% Rh	220	49
	400	56

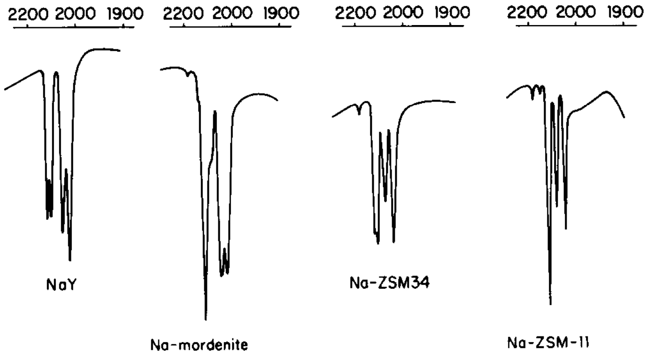

FIG. 1. Infrared spectra of $Rh(CO)_n$ species. Transmission vs frequency (cm^{-1}).

the exchanging species. We present here the essential features of the spectra; a more complete analysis of the different species produced by the reaction of CO on the Rh-zeolites will appear in a later publication.

In all four zeolites, two weak bands appear at ~2175 and ~2140 cm^{-1} which disappear upon exposure to vacuum. These bands are stable after heating in CO to 200°C except for Rh-Y. In agreement with Primet (*55*), we believe that these two species are of the type Rh(III)-CO where CO is bonded reversibly to a Rh(III) ion.

The other ir bands observed correspond to three Rh(I) carbonyl species which cannot be observed together. The characteristic frequencies of these bands are

Species **I**	2110 cm^{-1}	2020 cm^{-1}
Species **II**	2115 cm^{-1}	2045 cm^{-1}
Species **III**	2115 cm^{-1}	2085 cm^{-1}

The frequencies given above are average frequencies as the frequencies of each band vary slightly from one zeolite to the other. Table 6 lists the frequencies of all the Rh-CO species.

Species **III** is not stable under vacuum; it rapidly converts to species **II**. However, it is regenerated by the addition of CO.

A study using ^{12}CO–^{13}CO showed that **I** and **II** are dicarbonyl species. However, in the case of species **III**, some uncertainty exists as to whether it is a di- or tricarbonyl. In addition, when using EPR no Rh(II) could be detected.

These results, along with a recent study of Rh-Y (*56*), allow us to propose the structures for **I** and **II**:

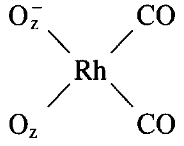

Species **I**

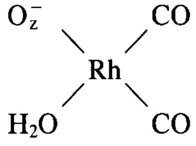

Species **II**

where O_z is a zeolite framework oxygen ion and O_z^- is a negatively charged zeolite framework oxygen ion.

For species **III** we propose the structure

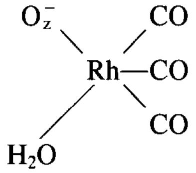

Species **III**

This new carbonyl species seems to form more easily as we go progressively from mordenite to ZSM-34 to ZSM-11. This series involves a progressive decrease in (1) Al content and (2) channel size. As the Al content diminishes, the electronic charge becomes more localized. This perhaps also explains the nonexistence of species **I** which is stabilized by resonance in Rh-Y and Rh-mordenite. The channel size may also play a role by allowing interaction between CO and the channel wall.

TABLE 6

Infrared Frequencies of Rh–CO Species

Species/Zeolite	Y	Mordenite	ZSM-34	ZSM-11
Rh(III)CO (1)	2172	2175	2188	2184
Rh(III)CO (2)	2138	2140	2140	2150
I $Rh(I)(CO)_2(O_z)_2$	2101–2022	2111–2016	Not observed	
II $Rh(I)(CO)_2(O_z)(H_2O)$	2116–2048	2111–2043	2113–2045	2116–2050
III $Rh(I)(CO)_3$	Not observed	2111–2083	2123–2080	2120–2085

DISCUSSION

Rh–X and Rh–Y zeolites have been prepared by numerous investigators (*17–40*) and have been studied as catalysts for the dimerization of ethylene (*17, 18, 30*), carbonylation of methanol (*19, 20, 23, 27, 29, 33*) and ethanol (*39*), the hydrogenation of ethylene and acetylene (*30*), the reduction of NO by CO (*35*), the hydroformylation and hydrogenation of ethylene and propylene (*38*), and the hydrogenation of CO (*40*) (see Table 7). Preparation methods for Rh–X and Rh–Y have generally included impregnation with $RhCl_3$ and exchange with either $[Rh(NH_3)_5Cl]Cl_2$ or $RhCl_3$ solutions. The samples prepared with the pentammine solutions were shown to have higher dispersion and to be more active in methanol carbonylation than those prepared from $RhCl_3$ solutions (*33, 34*). It was generally concluded that the use of rhodium pentammine chloride solutions involves the ion $[Rh(NH_3)_5Cl]^{2+}$ and results in genuine ion exchange with ions distributed uniformly throughout the zeolite (*18, 20*). Pentammine exchange has the advantage of avoiding zeolite damage because of the relatively high solution pH but the disadvantage that the NH_3 and Cl must be carefully removed to provide zeolites which, after H_2 reduction, contain highly dispersed Rh^0 with particle size <15 Å. The use of $RhCl_3$ or Rh $(NO_3)_3$ solutions has the potential advantage of avoiding the presence of the NH_3 ion but according to Refs. (*31, 34, 36*) results in a considerable proportion of Rh on the external surfaces of the zeolite. However, in these cases Rh was introduced by impregnation (*31, 34*) or by exchange with $RhCl_3(aq)$ at 25°C. Okamoto carried out exchanges in 0.013 *N* $RhCl_3(aq)$ at 90°C but did not determine whether the Rh was uniformly distributed throughout the zeolite. He postulated an exchange which involves $Rh(H_2O)_x^{3+}$, $RhCl(H_2O)_x^{2+}$, and hydroxo complexes based on uv spectra of the exchanged zeolites and Cl/Rh ratios of 0.4–0.6 determined by XPS (*30*).

Recent ^{103}Rh NMR studies show that the species $[Rh(H_2O)_4Cl_2]^+$ and $Rh(H_2O)_3Cl_3$ predominate in $RhCl_3(aq)$ solutions after equilibration at 80°C (*57*). The presence of a mixture of species was also noted earlier by Palmer and Harris (*58*) and Wolsey *et al.* (*44*). Meyer and Kawczyk (*59*) and Meyer and Kienitz (*60*) noted that only dilute solutions turned yellow on heating to 90–100°C and that the yellow solution contains free Cl^- ions, suggesting that heating decreases the concentration of the species richer in Cl. The progressive blue shift of the $[Rh(H_2O)_{6-n}Cl_n]^{3-n}$ absorption bands from 475 to 400 nm as n decreases from 3 to 0 is responsible for the color change (*44*). These results suggest that zeolite exchange in $RhCl_3$ solutions depends strongly on temperature and concentration. The fact that most previous investigators using $RhCl_3$ (aq) solutions used impregnations, lower temperatures, and more concentrated solutions (in those cases where the conditions are known) explains why their samples contained considerable Rh on the external surface whereas in this study homogeneous dispersions of Rh in Y were found. It would appear from our results that the same high dispersion and good methanol carbonylation activity found for pentammine-exchanged Rh–Y should be obtainable from $RhCl_3$(aq) exchange using dilute solutions and temperatures of 80–90°C.

Our XPS results demonstrate clearly that despite the presence of species with $n = 3$ as evidenced by a characteristic uv spectrum, the exchanging species in $RhCl_3$(aq) solutions contained only a small amount of Cl. Two possible explanations for this behavior are (1) the increased selectivity for trivalent ions relative to that for divalent ions (*61*) and (2) the sizes of the exchanging ions. Because the species $[Rh(H_2O)_{6-n}Cl_n]^{3-n}$ with $n = 1$ or 2 would be a relatively larger ion $d_{Rh}(1.3\ \text{Å}) + d_{H_2O}\ (2.8\ \text{Å}) + d_{Cl}\ (3.6\ \text{Å}) = 7.7\ \text{Å}$, assuming a hard-sphere model and typical ionic radii (*62*) and that Cl is perhaps not strongly attached to Rh, the Cl ion might be stripped from the complex and the exchanging ion could be $Rh(H_2O)_6^{3+}$ ($d \cong 6.9$ Å). The very similar XPS/CA analyses for ZSM-34 and ZSM-11 exchanged in both $RhCl_3$(aq) and $Rh(H_2O)_6^{3+}$ solutions support this hypothesis. Another possibility is that at pH 3.5–5.0 sufficient OH^- ions are present to produce $[Rh(H_2O)_{6-m}(OH)_m]^{3-m}$ ions which would also enter the zeolite channels easily. In a similar system Wan and Lunsford have recently shown that $[Ru(H_2O)_5OH]^{2+}$ exchanges into Y at pH 3.8 (*63*).

Similar considerations apply to exchanges involving $[Rh(NH_3)_5Cl]^{2+}$. High-temperature exchanges favor lower Cl/Rh ratios. However, in the case of the pentammine exchanges, the Cl seems to be more strongly bound than in the aquo complexes. Even in the smaller pore zeolites ZSM-34 and ZSM-11 where the degrees of exchange are considerably less than those for $RhCl_3$(aq) exchange, the Cl contents are not significantly less than those of the larger pore zeolites Y and mordenite.

Channel sizes in Y, mordenite, ZSM-34 and 11, erionite, A, and ZK-5 decrease from 7.4 Å for Y to 3.9 Å for ZK-5 (*64*) (see Table 1). The extent of exchange of $[Rh(NH_3)_5Cl]^{2+}$ and $Rh(H_2O)_6^{3+}$ in this zeolite series can generally be understood from the changing channel sizes relative to the sizes of the exchanging ions as defined by traditional ionic radii.

The ions $[Rh(NH_3)_5Cl_{1-n}(H_2O)_n]^{2+n}$ ($d_{Rh}\ (1.3\ \text{Å}) + 2d_{NH_3}(2.9\ \text{Å}) \cong 7.1\ \text{Å}$) and $Rh(H_2O)_6^{3+}$ ($d \cong 6.9$ Å) enter only the channels of Y easily, i.e., XPS/CA = 1.0 and most of the Rh in solution was exchanged. Although little or no Rh was found on the external surface of mordenite, suggesting facile exchange, there was only ~75% exchange with $Rh(H_2O)_6^{3+}$. ZSM-34 took up only ~35% of the $[Rh(NH_3)_5Cl_{1-n}(H_2O)_n]^{2+n}$ in solution and some of this was found on the surface. Almost all of the exchange must have occurred in the 6.4-Å channels because erionite, with the same secondary channel system (3.6 × 5.2 Å), exchanged little or no Rh. The smaller size of $Rh(H_2O)_6^{3+}$ vs the pentammine ion was reflected by the fact that twice as much Rh was exchanged. ZSM-11 with its smaller channels (5.1 × 5.5 Å) only exchanged 25% of the $[Rh(NH_3)_5Cl_{1-n}(H_2O)_n]^{2+n}$ in solution but 75% of the smaller ion $Rh(H_2O)_6^{3+}$ in $RhCl_3$(aq). The difference between ion exchange levels of the $RhCl_3$(aq) and $Rh(H_2O)_6^{3+}$ solutions is probably a result of the shorter exchange times for $Rh(H_2O)_6^{3+}$.

The relative proportions of Rh in the channels and on the exterior surface of ZSM-34 (XPS/CA = 1–2) and ZSM-11 (XPS/CA = 4–5) does not seem to depend on whether the exchanging ion is the pentammine or the hexa-aquo complex. Efforts to exchange Rh into all three zeolites with channels smaller than 4 Å, A, ZK-5, and erionite resulted in large quantities of Rh on the external surfaces (XPS/CA = 13–60).

Because of the fact that the pentammine

TABLE 7

Preparation of Rh–X and Rh–Y Zeolites

Sample	Rh Content, %	Exchange medium	Soln concn.	pH	*T*, °C	Time, hr	Comments	Reference
Na–Y	~7	$RhCl_3$	.03 *N*	3.6	70		• Used for ethylene dimerization	*17, 18*
Na–X	0.05–20.0	$RhCl_3 + NH_4OH$	Impreg	4.5	—		• Used for methanol carbonylation	*19*
Na–Y	0.5	$Rh(NH_3)_5Cl_3$	—	8–9	20	24	• Used for methanol carbonylation	*20*
Na–Y	3.1	$Rh(NH_3)_5Cl_3$	—	—	70–80	6	• EPR study of Rh(II) as function of *T* of treatment	*21*
Na–Y	0.2–10.0	$Rh(NH_3)_5Cl_3$	—	—	60–80	3	• EPR study of Rh pairs and interaction with H_2O, D_2O, NH_3, O_2	*22*
Na–X	~1	$RhCl_3$	Impreg?	—	80	15	• Used for carbonylation of methanol, ethanol, and propan-2-01	*23*
Na–Y	3.1	$Rh(NH_3)_5Cl_3$	.0007 *N*	—	80	12	• After O_2 (350°C), H_2 (500°C) 5–10 Å Rh^0 • Formation of $Rh(CO)_2$	*24*
Na–Y	6.0	$Rh(NH_3)_5Cl_3$	~.004 *N*	—	25	4	• Cl/Rh = 1; N/Rh = 5 (XPS) • Formation of Rh(III) CO and Rh(I) $(CO)_2$	*25*
Na–Y	2.8	$Rh(NH_3)_6(NO_3)_3$	—	—	60–80	3	• EPR study of NO adsorption on Rh pairs	*26*
Na–Y	0.4	$RhCl_3$	—	5.3	80		• Used for methanol carbonylation	*27*
Na–Y	2.2	$Rh(NO_3)_3$	~.0002 *M*	—	—		• Used for $4CO + 2H_2O \rightarrow CH_4 + 3CO_2$	*28*
Na–Y	0.3–7.0	$RhCl_3$	—	4.5	80		• Used for carbonylation of methanol	*29*
		$Rh(NO_3)_3$	—	4.5	80		• Studied effects of Rh content and exchange medium	
		$Rh_2(SO_4)_3$	—	4.5	80			
Na–Y	~1.9 ~5.4	$RhCl_3$	.013*N*	—	90	2–4	• Cl/Rh ≅ 0.4 (XPS); Cl removed between 150 and 300°C under vacuum • Cl/Rh ≅ 0.6 (XPS) • Used for hydrogenation of ethylene and acetylene and dimerization of ethylene • Rh(I) produced under vacuum at 250°C	*30*

Na–X	0.6	$RhCl_3$	Impreg?	—	80	15	• XPS and ir studies of Rh–X with and without CO • Rh/Si(XPS) = 0.05; Rh/Si(CA) = 0.01; Rh at surface. Cl/Rh = .18; Na/Si = 1/2 of expected • Rh reduced by X rays	*31*
Na–Y K–A		$RhBr_3$					• Rh–Y reduced under vacuum at 300°C • Probably hydrolysis to give $Rh(OH)_3$ ppt on A; $Rh(OH)_3$ on A did not reduce under vacuum	*32*
Na–X	0.6	$Rh(NH_3)_5Cl_3$	—	—	—	—	• Used for methanol carbonylation; more active (100×) than $RhCl_3$–Y	*33*
Na–X	0.6	$Rh(NH_3)_5Cl_3$	—	—	40–50	2–4	• Cl : Rh = 1, N : Rh = 5.3; Rh reduced by X-ray beam	*34*
	0.6	$RhCl_3$	Impreg.		25		• Cl : Rh = 0.11; Rh reduced less by X-ray beam; highly dispersed Rh^0 shows higher BE than bulk Rh^0; similar to Pt; Rh^0 at external surface of $X(RhCl_3)$ has lower BE than Rh^0 internal in X	
Na–Y	1.8	$Rh(NO_3)_3$	.01 *M*	—	80	—	• Used for reduction of NO by CO	*35*
	1.3	$Rh(NO_3)_3$	.004 *M*	4	80	—	• Rh(I) is dominant in active catalyst	
Na–Y	2	$Rh(NH_3)_5Cl_3$	—	4	80		• Rh/Si (XPS) = .023; Rh/Si (CA) = .020; XPS/Ca ≅ 1.1 • TPR reduction from 50 to 100°C	*36*
Ca–Y	2	$Rh(NH_3)_5Cl_3$	—	4	80			
Na–Y	0.5–4.0	$Rh(NO_3)_3$	—	4	80		• Rh/Si (XPS) = 0.13; Rh/Si (CA) = .018; XPS/Ca = 7.2, considerable Rh on surface • Above samples used in reaction $CO + H_2O \rightarrow CH_4 + CO_2$ • TPR – reduction from 50 to 100°C	
Na–Y	0.5–5.0	$Rh(NH_3)_5Cl_3$	.003–.01 *M*	—	25	24	• Study of CO uptake and CO_2 production over untreated and oxidized zeolites • Oxidized Rh–Y contains Rh(III) as isolated cations and/or oxidic species • Reduction of unoxidized Rh–Y produces large particle Rh 46–80 Å	*37*

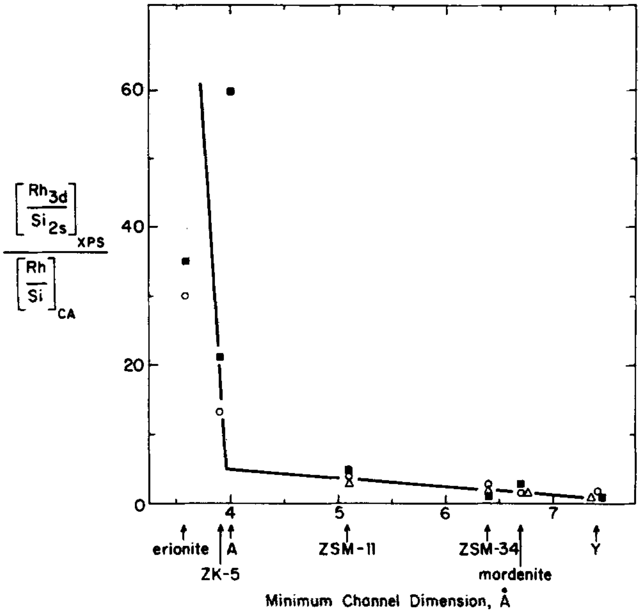

FIG. 2. Surface to bulk Rh ratio vs zeolite minimum channel dimension. ■, $RhCl_3(aq)$ exchange; ○, $Rh(H_2O)_6^{3+}$ exchange; △, $[Rh(NH_3)_5Cl]^{2+}$ exchange.

complex and hexa-aquo ions both have larger diameters than the channel openings of ZSM-34 and ZSM-11, it is apparent that the use of traditional ionic radii requires the concept of ion stripping (*64*) during the exchange process. The lack of exchange in the small-pore zeolites implies that at least one H_2O molecule cannot be stripped. This is consistent with the diameter of an ion (4.1 Å) formed from Rh^{3+} and one or two H_2O molecules.

The Rh on the external surfaces must result from hydrolysis of the aquo complexes which probably occurs because of an increase in pH at the zeolite surface. Figure 2 shows a plot of the XPS/CA ratios as a function of the smallest channel dimension in each zeolite. The relative amount of Rh at the external surface increases gradually as the channel size diminishes up to the small-pore zeolites where an abrupt increase occurs. This behavior can be interpreted in terms of simultaneous exchange and slow hydrolysis. If the complexes rapidly enter the channels, very little hydrolysis occurs, but if the exchanging complexes enter only with difficulty, proton exchange and subsequent slow hydrolysis result in increasing quantities of Rh on the external surface in the form of Rh oxide–hydroxides. In the case of the small-pore zeolites, little or no exchange occurs so that we have only a pure hydrolysis product. It is surprising, however, to see that pentammine exchange results in the same relative amounts of hydrolysis products. It was already noted that the Rh hydrolysis product behaves differently from precipitated $Rh(OH)_3$ in that, although both products are yellow, the precipitated material turns brown on heating at 110°C whereas the hydrolyzed product remains yellow.

The nature of the hydrolysis product is not precisely known. It is probably a Rh–oxy-hydroxy hydrate, identified as $Rh_2O_3 \cdot 5H_2O$ or $Rh_2O_3 \cdot H_2O$ by Miguelez (*66*). It deposits on the surface of a Rh–ZK-5 (3.5% Rh) in the form of regularly dispersed islands about 20–40 Å in diameter (see Fig. 3). Upon heating the sample for 3 hr in air at

FIG. 3. Transmission electron micrograph of Rh–ZK-5 (3.5% Rh).

550°C, these islands increase in size to ~30–45 Å and upon further heating in air for 1 hr at 750°C to 250–500 Å.

Diffuse reflectance spectra show bands at 260 and 440 nm similar to those of all zeolites exchanged in $RhCl_3$(aq) and $Rh(ClO_4)_3$ (aq). Thus the hydrolysis product is similar in nature to the species exchanged into the zeolite in that they both have O^{2-}, OH^-, or H_2O ligands. However, the hydrolysis product most likely contains a larger amount of OH^-.

Hydrolysis effects were noted by Schoonheydt *et al.* (*16*) in Ni–Y and Cu–Y and by Dyer and Barri (*15*) in Cu,Na–X. The former authors were not able to detect a second phase by X-ray diffraction but assumed a hydroxylated species on the basis of DTA endotherms at ~675°C for Ni–Y and at ~615°C for Cu–Y. Dyer and Barri observed $Cu_2(OH)_3NO_3$ precipitates in Na, Cu–X (*15*).

SUMMARY

Attempts to exchange Rh into zeolites of differing pore size results in simultaneous exchange and slow hydrolysis. In larger pore zeolites, such as Y and mordenite, exchange predominates. In medium-pore zeolites both exchange and hydrolysis on the zeolite external surface occur, whereas in small-pore zeolites hydrolysis predominates. The exchanging species in $RhCl_3$(aq) solutions at 90°C is apparently $Rh(H_2O)_6^{3+}$. Rh^0–Y with 90% dispersion can be prepared by heating $Rh(H_2O)_6^{3+}$–Y directly in H_2 at 200°C and omitting the preoxidative treatment used in $Rh(NH_3)_5Cl$–Y.

The carbonyl species obtained from reaction of CO with Rh–zeolites depends on the zeolite channel size: RhI $(CO)_2(O_z)_2$ in Y and mordenite; RhI $(CO)_2(O_z)$ H_2O in Y, mordenite, ZSM-34, and ZSM-11; and RhI $(CO)_3O_z$ in mordenite, ZSM-34, and ZSM-11.

ACKNOWLEDGMENTS

We thank H. Urbain and A. Chambosse for the Na and Al analyses; M. Dufaux for the hydrogen adsorption measurements; the Service Centrale d'Analyse du CNRS-Solaize for the Cl analyses; M. Van Kavelaar for the scanning electron micrographs; M. Bonnet for providing a sample of $Rh_2Cl_2(C_8H_{12})_2$; L. Abrams for providing the zeolite external surface areas; and P. E. Bierstedt for XPS analysis of the $RhCl_3 \cdot H_2O$. We are especially indebted to M. Alario-Franco for the electron micrograph and the CNRS-Laboratoire de Cristallographie in Grenoble for the use of the electron microscope.

REFERENCES

1. Barrer, R. M., and Townsend, R. P., *J. Chem. Soc. Faraday I* 2650 (1976).
2. Kasai, P., and Bishop, R. J., *J. Phys. Chem.* **81,** 1527 (1977).
3. Coughlan, B., McCann, W. A., and Carroll, W. M., *J. Colloid Interface Sci.* **74,** 136 (1980).
4. Badran, A. H., Dwyer, J., Eumerides, N. P., and Manford, J. A., *Inorg. Chim. Acta* **21,** 61 (1977).
5. Novakova, J., Kubelkova, L., Wichterlova, B., Juska, T., and Dolejsek, Z., *Zeolites* **2,** 17 (1982).
6. Ono, Y., Suzuki, K., and Keii, T., *J. Phys. Chem.* **78,** 218 (1974).
7. Pearce, J. R., Mortier, W. J., Uytterhoeven, J. B., *J. Chem. Soc. Faraday I* **75,** 1395 (1979).
8. Elliott, D. J., and Lunsford, J. H., *J. Catal.* **57,** 11 (1976).
9. Gelin, P., Coudurier, G., Ben Taarit, Y., and Naccache, C., *J. Catal.* **70,** 32 (1981).
10. Suib, S. L., Zerger, R. D., Stucky, G. D., Emberson, R. M., Debrunner, P. G., and Iton, L. E., *Inorg. Chem.* **19,** 1858 (1980).
11. Chu, P., and Dwyer, F. G., *Abstr. Div. Pet. Chem. Amer. Chem. Soc. Mtg.* Las Vegas, March 1982.
12. Jeanjean, J., Djemel, S., Guilleux, M. F., and Delafosse, D., *J. Phys. Chem.* **85,** 4145 (1981).
13. Bolton, A. P., *J. Catal.* **22,** 9 (1971).
14. McDaniel, C. V., and Maher, P. K., *Zeol. Chem. Catal. ACS Monogr.* **171,** 285 (1976).
15. Dwyer, A., and Barri, S. A., *J. Inorg. Nucl. Chem.* **39,** 1061 (1977).
16. Schoonheydt, R. A., Vandamne, L. J., Jacobs, P. A., and Uytterhoeven, J. B., *J. Catal.* **43,** 292 (1976).
17. Yashima, T., Ebisawa, M., and Hara, N., *Chem. Lett.* 473 (1972).
18. Yashima, T., Ushida, Y., Ebisawa, M., and Hara, N., *J. Catal.* **36,** 320 (1975).
19. Nefedov, B. K., Sergeeva, N. S., Zueva, T. V., Shutkina, E. M., and Eidus, Y. T., *Izv. Akad. Nauk SSSR Ser. Khim.* **3,** 582 (1976).
20. Nefedov, B. K., Sergeeva, N. S., and Eidus, Y. T., *Izv. Akad. Nauk SSSR, Ser. Khim.* **10,** 2271 (1976).
21. Naccache, C., Ben Taarit, Y., and Boudart, M., *Mol. Sieves II, ACS Symp. Ser.* 40, 1977.

22. Atanasova, V. D., Shvets, V. A., and Kazanskii, *Kinet. Katal.* **18,** 753 (1977).
23. Christensen, B., and Scurrell, M. S., *J. Chem. Soc. Faraday Trans. I* **73,** 2036 (1977).
24. Kaufherr, N., Primet, M., Dufaux, M., and Naccache, C., *C.R. Acad. Sci.* C286, 131 (1978).
25. Primet, M., Vedrine, J. C., and Naccache, C., *J. Mol. Catal.* **4,** 411 (1978).
26. Atanasova, V. D., Shvets, V. A., and Kazanskii, V. B., *Kinet. Katal.* **20,** 518 (1979).
27. Takahashi, N., Orikasa, Y., and Yashima, T., *J. Catal.* **59,** 61 (1979).
28. Niwa, M., Iizuka, T., and Lunsford, J. H., *J. Chem. Soc. Chem. Commun.* 684 (1979).
29. Yashima, T., Orikasa, Y., Takahashi, N., and Hara, N., *J. Catal.* **59,** 53 (1979).
30. Okamoto, Y., Ishida, N., Imanaka, T., and Teranishi, S., *J. Catal.* **58,** 82 (1979).
31. Anderson, S. L., and Scurrell, M. S., *J. Catal.* **59,** 340 (1979).
32. Kuznicki, S. M., and Eyring, E. M., *J. Catal.* **65,** 227 (1980).
33. Scurrell, M. S., and Howe, R. F., *J. Mol. Catal.* **7,** 535 (1980).
34. Anderson, S. T., and Scurrell, M. S., *J. Catal.* **71,** 233 (1981).
35. Iizuka, T., and Lunsford, J. H., *J. Mol. Catal.* **8,** 391 (1980).
36. Niwa, M., and Lunsford, J. H., *J. Catal.* **75,** 302 (1982).
37. VanBrabant, H., Schoonheydt, R. A., and Pelgrims, J., *Stud Surf Sci. Catal.* **12,** pp. 61–69 (1982).
38. Arai, H., and Tominaga, H., *J. Catal.* **75,** 188 (1982).
39. Scurrell, M. S., and Hauberg, T., *Appl. Catal.* **2,** 225 (1982).
40. Arai, H., Hironaga, A., and Seiyama, T., *Nippon Kagaku Kaishi* **(2),** 192 (1982).
41. Rubin, M. K., Rosinski, E. J., and Plank, C. J., U.S. Pat. 4,086,186, April 25, 1978.
42. Chu, P., U.S. Pat. 3,709,979, Jan. 9, 1973.
43. Robson, H. E., U.S. Pat. 3,720,753, March 13, 1973.
44. Wolsey, W. C., Reynolds, L. A., and Kleinberg, J., *Inorg. Chem.* **2,** 463 (1963).
45. James, B. R., and Rempel, G. L., *Canad. J. Chem.* **44,** 233 (1966).
46. Forrester, J. S., and Ayres, G. H., *J. Phys. Chem.* **63,** 1979 (1959).
47. Jorgensen, C. K., *Acta Chem. Scand.* **10,** 500 (1956).
48. Coudurier, G., Decamp, T., and Praliaud, *J. Chem. Soc. Faraday Trans. I* **78,** 2661 (1982).
49. Scofield, J. H., *J. Electron Spectrosc.* **8,** 129 (1976).
50. Lamb, A. B., *J. Amer. Chem. Soc.* **61,** 699 (1938).
51. Anderson, S. L. T., Watters, K. L., and Howe, R. F., *J. Catal.* **69,** 212 (1981).
52. Contour, J. P., Mouvier, G., Hoogewys, M., and Leclere, C., *J. Catal.* **48,** 217 (1977).
53. Nefedov, V. I., Shubochkina, E. F., Kolomnikov, I. S., Baranovski, I. B., Kukolev, V. P., Golubnichaya, M. A., Shubochkin, L. K., Porai-Koshits, M. A., and Volpin, M. E., *Russ. J. Inorg. Chem.* **18,** 444 (1973).
54. Takagi, M., Kawai, T., Soma, M., Onishi, T., and Tamaru, K., *J. Catal.* **50,** 441 (1977).
55. Primet, M., *J. Chem. Soc. Trans. Faraday I* **74,** 2570 (1978).
56. Lefebvre, F., and Ben Taarit, Y., *Nouv. J. Chim.*, in press.
57. Mann, B. E., and Spencer, C., *Inorg. Chim. Acta* **65,** L57 (1982).
58. Palmer, D. A., and Harris, G. M., *Inorg. Chem.* **14,** 1316 (1975).
59. Meyer, J., and Kawczyk, M., *Z. Anorg. Allg. Chem.* **228,** 297 (1936).
60. Meyer, J., and Kienitz, H., *Z. Anorg. Allg. Chem.* **242,** 281 (1939).
61. Barrer, R. M., and Klinowski, J., *J. Chem. Soc. Faraday I* 2080 (1974).
62. Shannon, R. D., *Acta Crystallogr. Sect. A* **32,** 751 (1976).
63. Wan, B-Z., and Lunsford, J. H., *Inorg. Chim. Acta* **65,** L29 (1982).
64. Meier, W. M., and Olson, D. H., *Adv. Chem. Ser.* **101,** 155–170 (1971).
65. Rees, L. V. C., *Annu. Rep. Prog. Chem. Sect. A* **67,** 191 (1970).
66. Miguélez, E. M., Ph.D. thesis, University of Madrid, 1982.